Dokuz Eylül Üniversitesi Mühendislik Fakültesi Fen ve Mühendislik Dergisi
Dokuz Eylul University Faculty of Engineering Journal of Science and Engineering
Elektronik/Online ISSN: 2547-958X

RESEARCH ARTICLE / ARAŞTIRMA MAKALESI

Fatigue Properties of Zinc Coated Low Carbon Steel Sheet Joints by the Means of Spot Welding

Çinko Kaplı Düşük Karbonlu Çeliklerin Nokta Kaynak Bağlantılarının Yorulma Özellikleri

Ahmet Çetkin *

Afyon Kocatepe Üniversitesi Teknoloji Fakültesi Makina Mühendisliği Bl., Afyonkarahisar, TÜRKİYE
Corresponding Author / Sorumlu Yazar *: acetkin@aku.edu.tr

Abstract

EN 10346:2015 DX52D+Z steel is a low-carbon, zinc-coated steel suitable for cold forming, widely used in the automotive industry due to its superior formability despite its low strength. Sheets produced in different sizes and forms are annealed by passing through the continuous galvanizing line after cold rolling. In this study, fatigue properties of these steels which were joined by spot welding with low welding current and high welding cycles, were measured and failure characterization was made, too. Tensile testing was made using a number of lap joints with different parameters and the variation of hardness within the weld area was also investigated. During the fatigue testing, crack initiation and propagation have been experimentally determined. A significant increase in hardness was observed from the base metal to the weld nugget, and the welding process caused a 38% reduction in the strength of the base material due to the heat affect from the joint. In the microhardness test, the highest hardness value was measured in the weld nugget heat affected zone (228.4 HV), and the hardness of the base metal was 169.4 HV. It has been determined that welded joints have infinite life below approximately 20% of the maximum tensile load.

Keywords: *Low carbon steel, Spot welding, Low welding current, High welding cycles, Fatigue limit*

Öz

EN 10346:2015 DX52D+Z, düşük mukavemetine rağmen üstün şekillendirilebilirliği nedeniyle otomotiv endüstrisinde yaygın olarak kullanılan, düşük karbonlu, soğuk şekillendirmeye uygun çinko kaplı bir çeliktir. Farklı ebat ve formlarda üretilen saclar, soğuk haddeleme sonrası sürekli galvanizleme hattından geçirilerek tavlanmaktadır. Bu çalışmada düşük kaynak akımı ve yüksek kaynak çevrimi ile nokta kaynağı ile birleştirilen bu çeliklerin yorulma özellikleri ölçülerek hasar karakterizasyonları da yapılmıştır. Farklı parametrelere sahip bir dizi bindirmeli bağlantı kullanılarak çekme testi yapılmış ve kaynak bölgesindeki sertlik değişimi de incelenmiştir. Yorulma testi sırasında çatlak başlangıcı ve ilerlemesi deneysel olarak belirlenmiştir. Ana metalden kaynak çekirdeğine kadar sertlikte önemli bir artış gözlenmiş ve kaynak işlemi, birleştirmeden gelen ısı etkisinden dolayı ana malzemenin mukavemetinde %38'lik bir azalmaya neden olmuştur. Mikrosertlik testinde en yüksek sertlik değeri kaynak çekirdeğinin ısıdan etkilenen bölgesinde (228.4 HV) ölçülmüştür ve ana metalin sertliği 169.4 HV olmuştur. Kaynaklı bağlantıların maksimum çekme yükünün yaklaşık %20'sinin altında sonsuz ömre sahip olduğu belirlenmiştir.

Anahtar Kelimeler: *Düşük karbonlu çelik, Nokta kaynağı, Düşük kaynak akımı, Yüksek kaynak döngüleri, Yorulma limiti*

1. Introduction

Spot welding is the most important joining technique in the production of basic parts of the vehicles, such as the chassis, it is mostly associated with automotive manufacturing. In addition to the developments on the spot welding method, other joining methods are also in the process of making continuous progress in the manufacture of the body and bodywork, such as laser spot welding [1]. It is mostly significant in the automotive and white goods sectors that studies on safety of passengers and the weight reduction on the vehicle have led to the use of different materials together and ultimately search for a different manufacturing method. However, the most important joining method in the manufacture of vehicles is still the electric resistance spot welding method. Compared to other methods in production of vehicles, the rate of use of spot welds in the vehicle body is around 85% and an average of 3,000 to 5,000 spot welds are made on the bodywork of the vehicles [2].

Many studies on issues such as eliminating the basic problems encountered during the application of spot welding, obtaining more effective results with changes in parameters, new applications in spot welding techniques, etc. have continued to advance from the first days until today [3-11]. Spot welding problems such as welding spatters, the degradation of the electrode tip causing short electrode life, a decrease in strength due to misalignment, shunt current loss between welded points, welding of more than two sheets, spot welding of different metals such as aluminum and steel sheets, surface coatings, surface oxides and surface contact resistance etc. problems have been extensively studied [12- 20].

DOI:10.21205/deufmd.2024267714

Atıf şekli / How to cite:

Cetkin, A. (2024). Fatigue Properties Of Zinc Coated Low Carbon Steel Sheet Joints By The Means Of Spot Welding. DEUFMD, 26(77), 299-306.

Geliş Tarihi / Received: 28.02.2023
Kabul Tarihi / Accepted: 25.10.2023

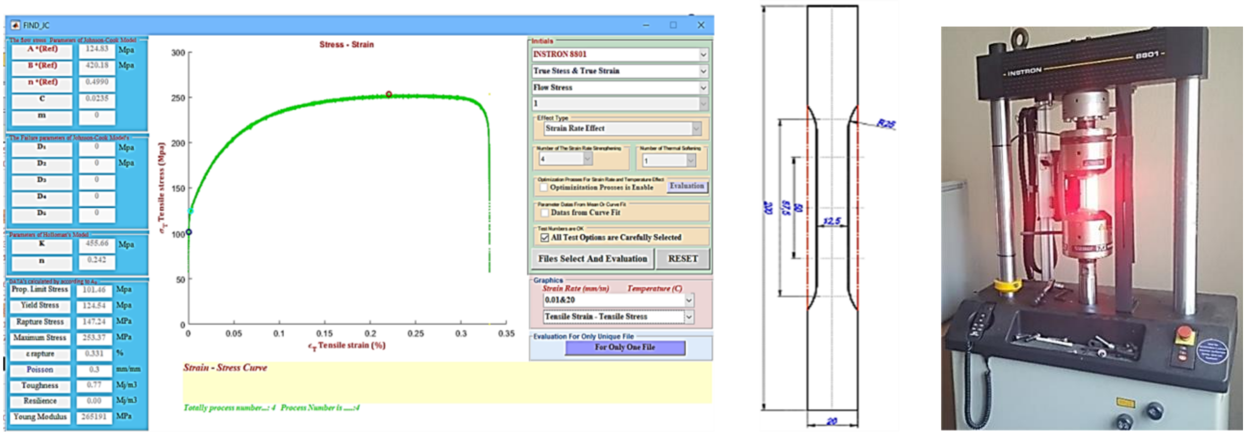

(a) (b) (c)

Figure 1. a) Software interface, b) Tensile test specifications and c) Quasi-static tensile test machine

Table 1. Mechanical properties of EN 10346:2015 DX52D+Z steel

			Holloman Plasticity Model Coefficient		Johnson-Cook Plasticity Model Coefficient		
Yield Strength (MPa)	**Ultimate Strength(Mpa)**	**Total Elongation (%)**	**K**	**n**	**A**	**B**	**n**
124,54	253,37	33,1	455,66	0,242	124,83	420,18	0,499

Table 2. Chemical composition of EN 10346:2015 DX52D+Z steel

	Si%	**Mn%**	**P%**	**S%**	**Cr%**	**Mo%**	**Ni%**	**Nb%**
0.050	<0.001	0.249	0.006	0.028	0.034	0.014	0.041	<0.002
Al%	**Cu%**	**Co%**	**B%**	**Ti%**	**V%**	**W%**	**Sn%**	**Ca%**
0.165	0.030	0.014	0.0074	0.001	0.003	0.006	0.006	0.0027
As%	**Mg%**	**Ce%**	**La%**	**Pb%**	**Sb%**	**Te%**	**Zr%**	**Fe%**
0.013	0.0006	0.021	0.012	0.003	<0.005	<0.001	<0.001	99.291

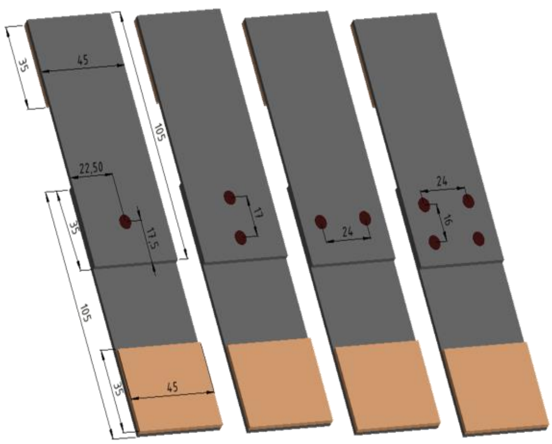

(a) (b) (c) (d)

Figure 2. Typical geometry of tensile shear spot welding samples including multi-points, a-Single point welded(OP), b-Welded from two vertical points(TVP), c-Welded from two horizontal points(THP), d-Four point welded(FP).

Many studies have also been conducted on the fatigue behaviour of different types of loading effects to evaluate the fatigue strength of spot weld joints [21-23]. Many different methods have also been proposed to estimate fatigue life of the spot-welded joints [24-26]. Using fracture mechanics approach that considers a nugget edge as a crack tip, the fatigue life of the joints was evaluated on the local stress around weld nugget and local strain in the vicinity of a weld nugget [27-32].

The aim of this study is to experimentally investigate the fatigue properties of plates joined to each other by spot welding of EN 10346:2015 DX52D+Z steel, which is preferred for its easy formability in the automotive industry. First of all, by keeping the other five important parameters (Electrode diameter, welding time, squeeze time, holding time and electrode force) constant, the welding current that creates the maximum tensile force was determined. The lap joints were produced with a single and multiple spot welds and tensile tested. The structure and size of the weld nugget, fatigue crack initiation and propagation were examined and fracture mechanisms related to the failure have been discussed.

2. Materials and Methods

2.1. Materials and methods subheading

The basic mechanical properties and chemical composition of EN 10346:2015 DX52D+Z steel are shown in Table 1 and Table 2, respectively. The tensile test samples (Fig. 1b) prepared according to EN ISO 6892-1 standards were tensile tested with the 8081-Instron universal servo-hydraulic testing machine (Fig. 1c) at a crosshead speed of 0.01 mm/s at room temperature in accordance with the standards. Here, the data from ten samples were calculated using software and the basic tensile test average data were obtained (Fig. 1a).

A semi-automatic spot welder (SIMSEK 50KA) was used for the welding process. Two sheets of 1 mm thickness were joined under pre-set PLC control parameters. For this sheet metal thickness, the recommended G-16 type copper alloy electrode caps were used for all spot welds. The diameter of the caps is 16mm and the diameter of the welding contact surface is 6mm. The overall dimensions of samples for fatigue tests are shown in Figure 2. The sheets were prepared and tested according to EN ISO 14273 (Specimen dimensions and procedure for shear testing of resistance spot welds); the samples were in dimensions of 45 x 105 mm and sliced parallel to rolling direction, and welded according to the dimensions determined by the standard. In specimens of shear type tensile fatigue test, two spacers of 45 mm length of the same thickness were mounted on the sample ends in order to reduce the bending effect. The two sheets to be welded were mounted together with 35 mm long surfaces. As it can be seen in Figure 2. that a combination of a single, double and quadruple spot welds were used in the tests; spacing between the spot welds and edges were determined with sufficient distance.

2.2. Optimal weld current procedure

Studies showed that the most important parameter for the optimum quality, strength and fatigue life of the weld joint is the form of the nugget that forms between the sheet metals during the spot welding process. [23, 33-35]. There are many spot welding parameters such as electrode diameter, current holding time, clamping time, electrode force, welding current etc. for the formation of the spot weld joint. The latter is the most significant parameter compared to other process parameters that determine the quality of the weld joint. If the welding current is too low, it is impossible to have sufficient heat generated to form the weld nugget and hence low mechanical properties are inevitable. Even if a nugget is formed, it may cause a low strength because of spot weld nugget considerably smaller than the minimum nugget diameter [36, 37]. When the current is high, there is a risk of over melting the entire weld nugget region and result in a decreased thickness of nugget zone.

The basic principle in spot welding nugget formation is the contact resistance at the electrode-sheet and the sheet-sheet interfaces, playing a dominant role in the Joule heat generation encountered by the welding current as it passes from one electrode to the other. Hence, the heat is produced in proportion to the contact resistance of the region formed by the electrodes and plates [38], and the temperature increase in this region causes an increase in the overall resistance of this region. Melting in this zone firstly begins at the contact surface between the sheets and spreads into the other parts of the both sheets, leaving metallurgically affected base metal nearby nugget zone.

Electrode surface contact diameter was selected as a 6 mm and 30 cycles of weld time, 60 cycles of squeeze time, 30 cycles of holding time, 260 kP of electrode force. By keeping these parameters constant, an optimum the strength levels of the joints were attempted to obtain with the changing welding current. Tensile test of specimen joined with different welding currents

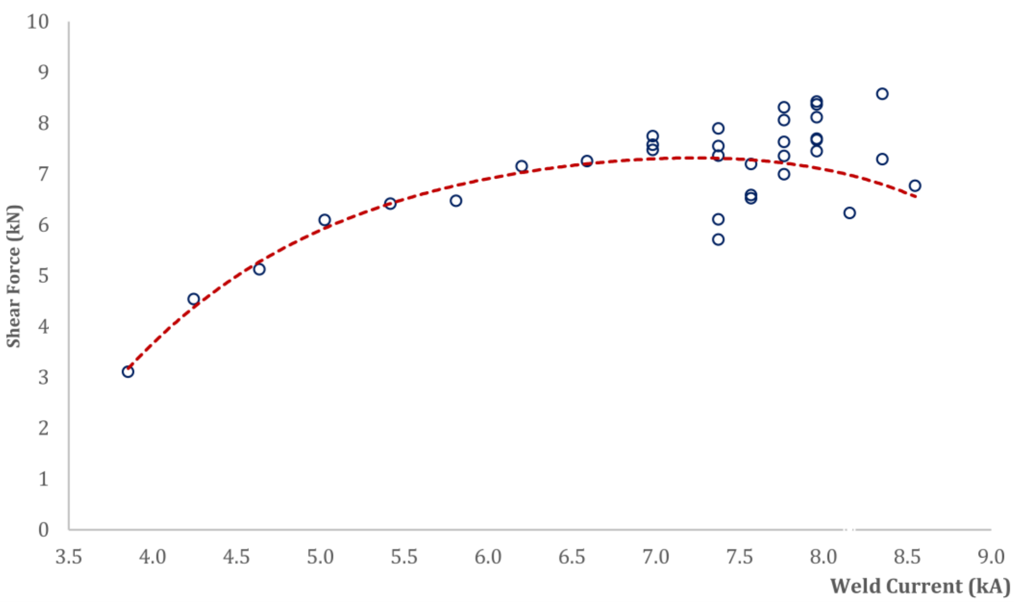

Figure 3. Shear load vs. weld current plot for optimal welding parameters choice

and consequent microscopic examination showed that 7.75 kA gives the best optimal shear force value for samples spot welded (Fig. 3).

The tensile shear test graph of three samples with different numbers of spot-welding combination produced by using 7.75 kA welding current is given in Figure 4; other parameters were kept constant. In order to determine the force for fatigue test, which is to be performed later, the shear force values were used by taking the average of 20 shear force-extension tests for each test.

When the stiffness exceeds the selected 25% value, the joint is now considered to be failed [39]. The testing was carried out and the results were calculated over the entire test values as in Figure 4 for a single weld point and for 33%-50%-66% of the average maximum shear force. As seen in Figure 5, it was determined that the stiffness value appeared from the upper value of 47% and slowly progressed downwards throughout the entire test. A large decrease was observed suddenly when the fatigue life reached 90-95% due to the growing fatigue cracks being unable to carry the load.

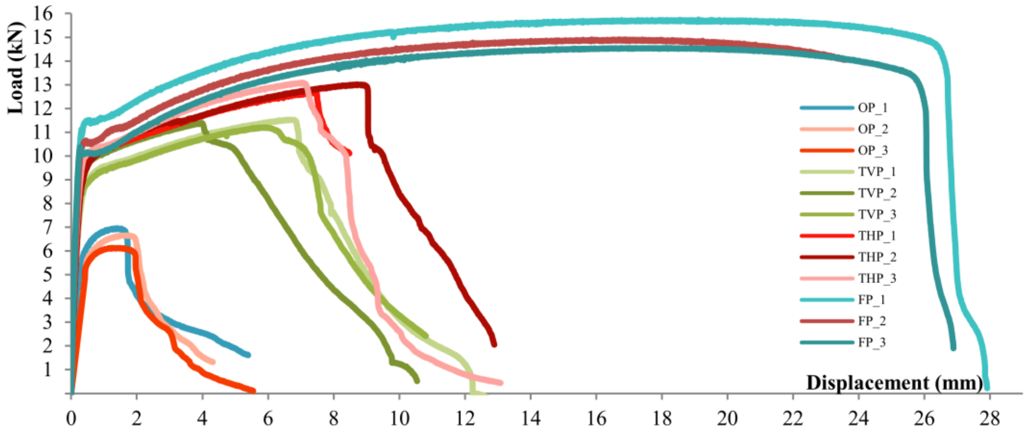

Figure 4. Shear load vs. weld current plot for optimal welding parameters choice

2.3. Fatigue test procedure

8801-Instron universal servo-hydraulic testing machine was used to conduct fatigue test on lap joint and non-welded test specimens. The spot-welded samples were subject to various sinusoidal load by using SAX software preloaded on the universal testing machine. Considering the sensitivity of the test device, R = 0.1 for load ratio and a test loading frequency of 25 Hz were used. In similar studies, the loading frequency was taken within the range of 5-25 Hz [39, 40]. The weld stiffness behaviour during fatigue loading test is observed in the force data obtained from load cell and the displacement data measured with an extensometer. For welded samples, the weld stiffness value is taken as 25% as given in the literature [39]. The stiffness value is the ratio of the differential force value to the displacement change during the test, and the results were evaluated after the tests.

2.4. Microstructure, fracture morphology observation and microhardness measurements

For microstructure and fracture morphology observation, all welded samples were longitudinally sliced along the center of the nugget. The cutting process was done manually on a Metkon Metacut-M250 precision cutting machine at high speed.

The sample was mounted for polishing using a thermosetting plastic compound. The cross-section of the samples was polished using sand-paper to 1 micron and then etched by holding it in 3% Nital etchant fluid for 3-3.5 seconds.

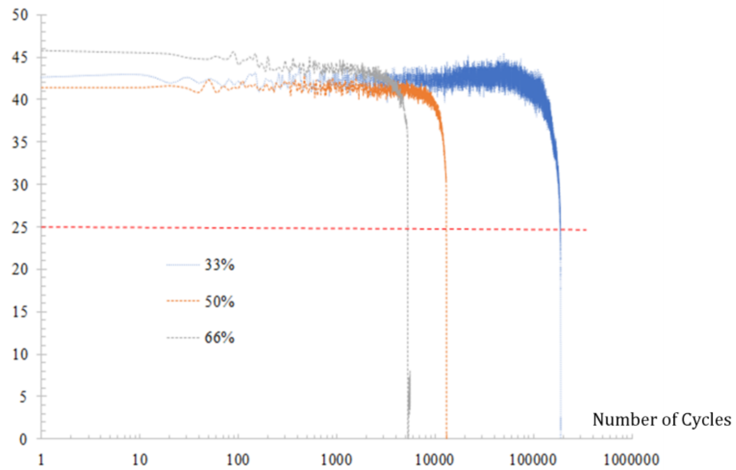

Figure 5. Stiffness ratio vs. number of cycles graphs for three fatigue load ratios

.

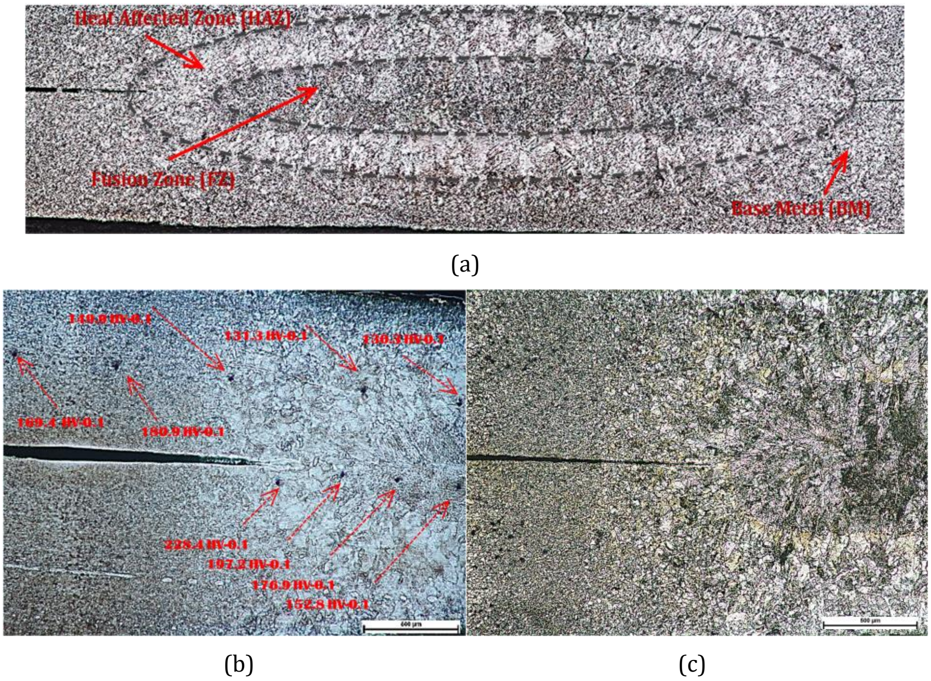

Figure 6. (a) Macrostructure of weld nugget and zones(Base Metal (BM), Heat Affected Zone (HAZ), Fusion Zone (FZ)) (b) Microhardness of weld nugget region, (c) Microstructure of weld nugget.

Vickers hardness tests were performed with a 100 g load using Mikrobul low load Vicker hardness tester, on the surface of the polished specimens. In addition, the measurement was made along a line parallel to the sheet contact area and at a distance of 850 µm in order to make measurements in the base metal area with localized microstructural changes took place in the weld area in Figure 6; hardness values, microhardness indentations and the distances between them is also given in Figure 6.

Half and symmetrical weld nugget is shown in Figure 6a. The hardness values measured here are also symmetrical with other side of the welding. The three typical microstructures in the welded joint region are called base metal(BM), fusion zone (FZ) and heat affected zone (HAZ) [Fig. 6a]. The heat affected zone (HAZ) and the base metal (BM) are clearly separated and this separation is clearly determined by the microhardness test. In Figure 6a, it can be seen that a hardness of approximately 152.8 HV-0.1 in the weld nugget and 169.4 HV-01 in the base metal were measured, and hardness reaching the highest value in the near region of the line separating the weld nugget and the base metal with 228.4 HV-0.1.

The ferritic-martensitic structure seen in the welding nugget of low carbon steels and the heterogeneous appearance in the HAZ, which is also confirmed by hardness measurement, are given in Figure 6b. In some studies, it has been determined that the formation of martensite in the welding area of this type of steel is due to the quenching effect of copper alloy electrodes and their quenching effect, as well as the short welding cycle. In these FE technique studies [41-44] in which the weld joint was modeled, it was calculated that even the 1000 °C/s cooling rate required for martensite formation was exceeded. As seen in Fig 6c, as in similar studies, the HAZ structure in the region close to the fusion boundary consists of martensite, grain boundary ferrite and Widmanstatten ferrite [45].

3. Results

The fatigue life curves of EN 10346:2015 DX52D+Z steel are shown in Figure 7. Infinite life values for the spot-welded joints (Fig. 7) are taken according to the maximum shear force (Figure 4). The % ratio of test results is given in Figure 8. The forces were divided into ten equal parts and applied on the samples prepared in accordance with the standard. It was assumed that it would reach an infinite lifetime when the number of cycles exceeded 1E+7.

Each data sets having different type or number weld point could be characterized by similar smooth curves as in Fig. 7 and Fig. 8. For test specimens with four different number of spot weld joints, changes were observed according to the nature of the force magnitude and the life limits were found to be similar based on the load amplitude ratio %. As a result of the tests, it was observed that the fatigue strength was approximately 20% of the static joint strength. The static strength values used here were obtained by averaging more than twenty quasi-static tensile shear tests (Test speed=0.01 mm/s) for each sample containing a different number of spot welds. The life curves found by the least squares' method, which can be defined by the exponential equation, can be defined by the number of load cycles applied to the sample up to the values above the life limit (Fig. 7). In the equations obtained from the curve fitting, the average R-square of the curve-fit procedure was calculated as 98.2%

Fatigue cracks are encountered in a circular geometry in the sample around the weld at the sheet interface. This circular form is one of the most obvious indicators of stress concentration. Throughout the entire fatigue life, it is believed that the crack path was determined by the stress distribution around the weld as no preferred microstructural path was found [39]. Fatigue strength depends on the nature of the load on the spot weld and the stress concentration factor of the circumferential notch around the weld [21].

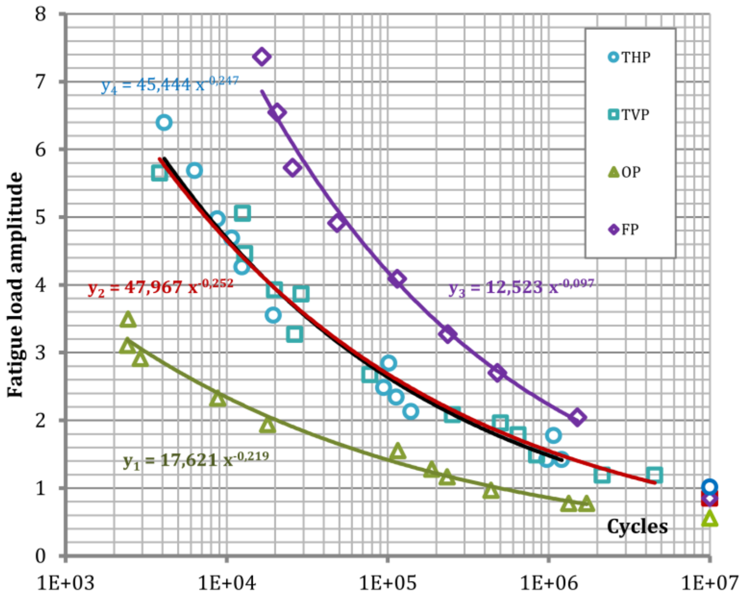

Figure 7. Fatigue load amplitude vs. cycles-to-failure curves for the tensile-shear samples

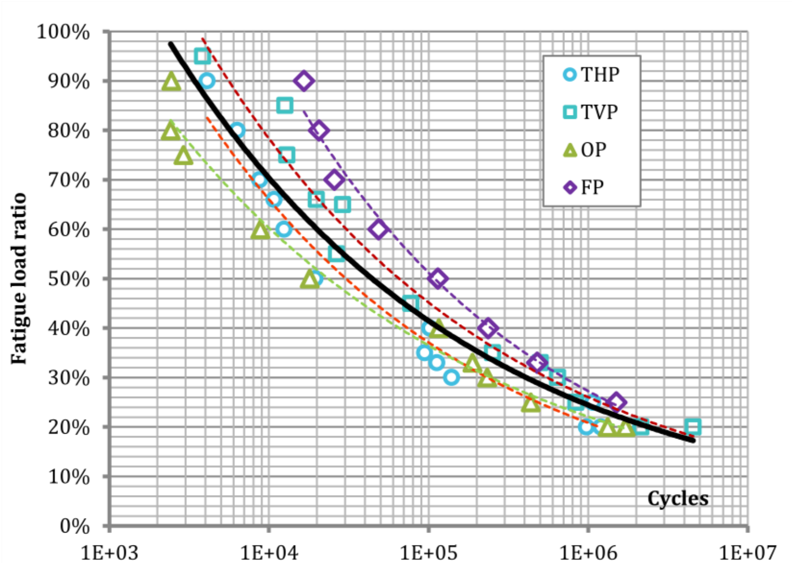

Figure 8. Fatigue load ratio vs. cycles-to-failure curves for the tensile-shear samples

Different types of failure modes can be associated with different separation load type and direction. Naturally, a similar type of failure mode was encountered in the tests. The samples exhibited a fracture morphology where the weld button remained intact on one sheet and separated from the other steel sheet. Fatigue crack was measured to occur at a distance of approximately 0.75 mm from the weld button. When a fatigue crack is first formed, the crack propagates partially along the thickness of the sheet and around the circumference of the weld button at a small angle. Then crack continues to expand perpendicular to the direction of pull as it propagates planarly along the plane towards the base sheet (Fig. 9).

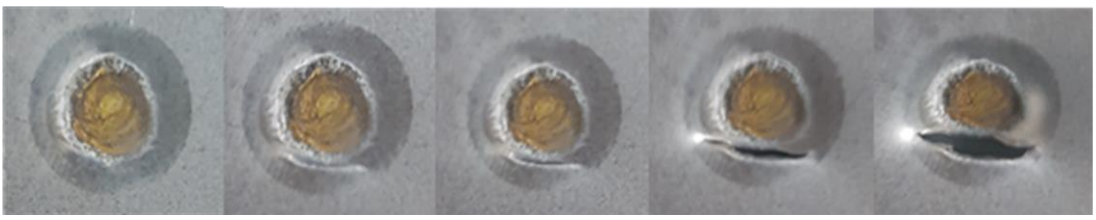

Figure 9. Development of crack propagation in %50 load amplitude ratio

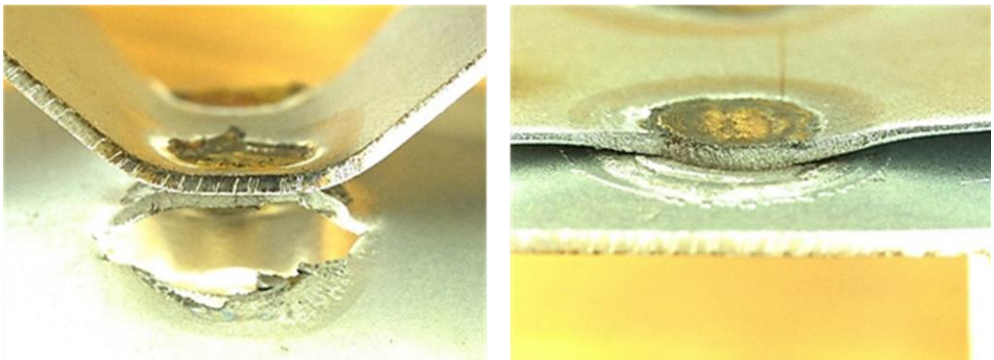

Figure 10. (a) Failure mode on one-spot welded joint; (b) Failure mode on four-spot welded joint

At this moment, the crack completely penetrates the thickness of the sheet. Now that the crack has fully penetrated the sheet thickness, the weld is further released and the tensile-shear specimen tends to rotate due to the unbalanced load distribution of the load. As a result, the specimen rotates slowly about an axis parallel to the tensile plane of the tester jaws (Fig. 10a), except for the four spot welded specimen by its nature (Fig. 10b).

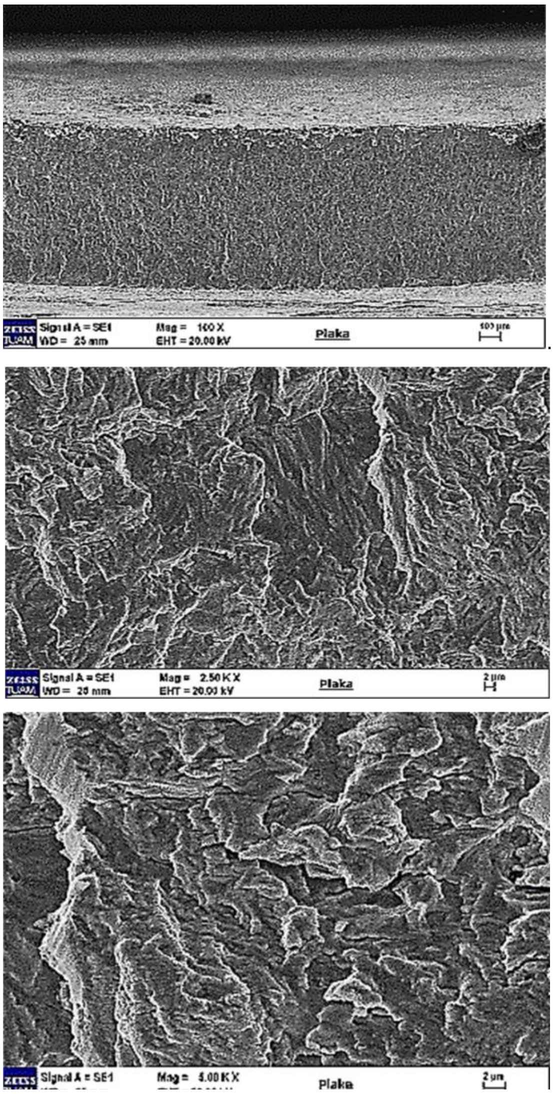

Figure 11. Microstructure of the crack surface of the welded joint with a squeeze time of 60 cycles and a welding current of 5.4 kA

Fatigue increases the stress triaxiality at the crack tip, thus further increasing the crack growth rate. The overall failure occurs by tearing of the base material due to the fact that it can no longer carry the increasing load with the effect of an additional moment applied at the crack tip.

Microstructures and fatigue crack surface morphologies are shown i Fig.10 and Fig. 11. As seen in Figure 11., both striation-like characteristic structure and non-uniform dimple-like structures were observed. This image suggests a ductile type of failure. Coarse columnar dendritic crystals (Fig. 6), which can be easily observed in the spot weld nugget, are surrounded by the heat affected zone, which has a boundary with different microhardness values from the base metal and weld nugget. After the fatigue load, the stress concentration forms a crack. Crack path is determined along the HAZ boundary, crack initiation and propagation are probably due to the interaction between plastic zone formation in this circumferential notch.

4. Discussion and Conclusion

An experimental investigation of the fatigue properties of EN 10346:2015 DX52D+Z steel spot welded samples led to the following conclusions:

1. Microhardness tests showed that a hardness of approximately 228.4 HV-0.1 in weld nugget boundary (HAZ), 169.4 HV-0.1 in base metal and 152.8 HV-0.1 in weld nugget.

2. The welding process caused a 38% decrease in the strength of the base material due to the joining by applied heat and its effect on the base metal, and it was observed that the fatigue strength was approximately 20% of the static strength.

3. Fatigue crack was measured to occur at a distance of approximately 0.75 mm from the weld button. When a fatigue crack is first formed, the crack propagates partially along the thickness of the sheet and around the circumference of the weld button at a small angle. Then crack continues to expand perpendicular to the direction of load as it propagates planarly along the plane towards the base sheet.

Ethics committee approval and conflict of interest statement

This article does not require ethics committee approval.

This article has no conflicts of interest with any individual or institution.

Acknowledgment

This work was supported by Afyon Kocatepe University, Scientific Research Projects Coordination Unit (18.FEN.BİL.65) Afyonkarahisar, Turkey.

References

[1] Li, M., Tao, W., Zhang, J., Wang, Y., Yang, S. 2022. Hybrid resistance-laser spot welding of aluminium to steel dissimilar materials: Microstructure and mechanical properties, Materials & Design, Volume 221, 111022, ISSN 0264-1275.

[2] Mallick, P.K. 2021. Chapter 8 - Joining for lightweight vehicles, In Woodhead Publishing in Materials, Materials, Design and Manufacturing for Lightweight Vehicles (Second Edition), Woodhead Publishing, Pages 321-371, ISBN 9780128187128, https://doi.org/10.1016/B978-0-12-818712-8.00008-2.

[3] Raut, M., Achwal, V. 2014, Optimization of Spot Welding Process Parameters for Maximum Tensile Strength, Int. J. Mech. Eng. & Rob. Res., 506-517.

[4] Holdren, R.L. 1993. What Are the Causes of and Solutions to Weld Quality Control, Welding Journal Vol. 72, No. 8.

[5] Hirsch, R.B. 1993. Tip Force Control Equals Spot Weld Quality, Welding Journal, vol. 72, No. 3.

[6] Cullison, A. 1993. Resistance Weld Controller Delivers the Heat Where It's Needed, Welding Journal, Vol. 72, No. 6.

[7] James, P.S. Chandler, H.W., Evans, J.T., Wen J, Browne, D.J., Newton, C.J. 1997. The Effect of Mechanical Loading on The Contact Resistance of Coated Aluminium, Materials Science and Engineering: A, Volume 230, Issues 1–2, Pages 194-201.

[8] Papkala, H. 1990. A New Method of Projection Welding of Galvanised Steel Sheet, Welding International, Volume 4, Issue 5 Pages 341-346.

[9] Papkala, H. 1992, Technological Problems in Spot Welding of Galvanized Car Body Sheet, Journal Welding International, Volume 6, Issue 5.

[10] Komizo, Y.I. 1987. Crack Susceptibility of Steel Plates Produced by The Thermo-Mechanical Control Process, Welding International, v.1, p.126-32.

[11] Patel, S. Reddy, P., Kumar, A. 2021. A Methodology to Integrate Melt Pool Convection With Rapid Solidification And Undercooling Kinetics In Laser Spot Welding, International Journal of Heat and Mass Transfer, Volume 164.

[12] Graham, S.L., Holzer, R.A., Gerbic, J.F. 2007. System and Method for Reducing Weld Spatter, US 20070284350 A1.

[13] Parshuramkar, N.T., Rambhad, K.S., Chandran, R. 2017. Welding Spatter Reduction and Time Study: A Review. International Journal of Analytical, Experimental and Finite Element Analysis (IJAEFEA). 4. 10.26706/IJAEFEA.4.4.20171025.

[14] Lum, I., Biro, E., Zhou, Y., Fukumoto, S., Boomer, D. 2004. Electrode Pitting in Resistance Spot Welding of Aluminum Alloy 5182. Metallurgical and Materials Transactions A. 35. 217-226. 10.1007/s11661-004-0122-8.

[15] Ma, N., Murakawa, H. 2010, Numerical and experimental study on nugget formation in resistance spot welding for three pieces of high strength steel sheets. Journal of Materials Processing Technology - J Mater Process Technol. 210. 2045-2052. 10.1016/j.jmatprotec.2010.07.025.

[16] Wang, B., Lou, M., Shen, Q., Li, Y., Zhang, H. 2013. Shunting effect in resistance spot welding steels - Part 1: Experimental study. 92. 182S-189S.

[17] Müftüoğlu, F., Keskinel, T. 2007. Effect of Coating Thickness on Electrode Life in the Spot Welding of Galvanized Steels, Turkish J. Eng. Env. Sci. 31, p,183 – 187.

[18] Tomoyuki, F., Keiichiro, T., Yukinori, S., Takahiro, Y., Yoshinobu, S. 2016. Fatigue strength and fatigue fracture mechanism of three-sheet spot weld-bonded joints under tensile–shear loading, International Journal of Fatigue, Volume 87, Pages 424-434, ISSN 0142-1123, https://doi.org/10.1016/j.ijfatigue.2016.02.023.

[19] Chen, Z., Zhou, Y., Scotchmer, N. 2006. Coatings on Resistance Welding Electrodes to Extend Life. SAE Transactions,115, 106-110., http://www.jstor.org/stable/44722317.

[20] Zou, J., Zhao, Q., Chen, Z. 2009. Surface modified long-life electrode for resistance spot welding of Zn-coated steel, Journal of Materials Processing Technology, Volume 209, Issue 8, Pages 4141-4146, ISSN 0924-0136, https://doi.org/10.1016/j.jmatprotec.2008.10.005.

[21] Long, X., Khanna, Z.K. 2007. Fatigue properties and failure characterization of spot-welded high strength steel sheet Int J Fatigue, 29, pp. 879-886.

[22] Wang, B., Duan, Q.Q., Yao, G., Pang, J.C., Li, X.W., Wang, L. 2014. Investigation on fatigue fracture behaviours of spot welded Q&P980 steel Int J Fatigue, 66, pp. 20-28.

[23] Vural, M., Akkuş, A., Eryürek, B. 2006. Effect of welding nugget diameter on the fatigue strength of the resistance spot welded joints of different steel sheets, Journal of Materials Processing Technology, Volume 176, Issues 1–3, Pages 127-132, ISSN 0924-0136, https://doi.org/10.1016/j.jmatprotec.2006.02.026.

[24] Pan, N., Sheppard, S. 2002. Spot welds fatigue life prediction with cyclic strain range, Int J Fatigue, 24, pp. 519-528.

[25] Hassanifard, S., Zehsaz, M., Tohgo, K., Ohguma, T. 2009. The prediction of fatigue crack initiation life in spot welds Strain, 45, pp. 489-497.

[26] Tanegashima, R., Akebono, H., Sugeta, A. 2017. Fatigue life estimation based on fracture mechanics of single spot-welded joints under different loading modes, Engineering Fracture Mechanics, Volume 175, Pages 115-126, ISSN 0013-7944, https://doi.org/10.1016/j.engfracmech.2017.01.031

[27] Nakayama, E., Miyahara, M., Okamura, K., Fujimoto, H., 2004. Fukui, K. Prediction of fatigue strength of spot-welded joints based on local material strength properties measured by small specimen, J Soc Mater Sci, Jpn, 53 (12), pp. 1136-1142.

[28] Tohgo, K., Ohguma, T., Shimamura, Y., Ojima, Y, 2009. Influence of strength level of steels on fatigue strength and fracture morphology of spot-welded joints, J. Soc. Mater. Sci, Jpn., 59 (7), pp. 627-634

[29] Bae, D.H., Sohn, I.S., Hong, J.K. 2003. Assessing the effects of residual stresses on the fatigue strength of spot welds, Weld. J., pp. 18s-23s.

[30] Lin, S.H., Pan, J., Wung, P., Chiang, J. 2006. A fatigue crack growth model for spot welds under cyclic loading conditions, Int J Fatigue, 28 (7), pp. 792-803.

[31] Ertaş, A.H., Yılmaz, Y., Baykara, 2008, C. An investigation of the effect of the gap values between the overlap portions of the spot-welded pieces on fatigue life, Proc. Inst. Mech. Eng., Part C: J. Mech. Eng. Sci., 222 (6), pp. 881-890.

[32] Dancette, S., Fabregue, D., Estevez, R. 2012. A finite element model for the prediction of advanced high strength steel spot welds fracture, Eng. Fract. Mech., 87, pp. 48-61.

[33] Nguyen, T.N., Wahab, M.A. 1998. The effect of weld geometry and residual stresses on the fatigue of welded joints under combined loading, J. Mater. Process. Technol., 77 (1–3), pp. 201-208.

[34] Kumar, A., Panda, S., Ghosh, G.K., Patel, R.K. 2020. Numerical simulation of weld nugget in resistance spot welding process, Materials Today: Proceedings, Volume 27, Part 3, pp 2958-2963, ISSN 2214-7853, https://doi.org/10.1016/j.matpr.2020.04.901.

[35] Eisazadeh, H., Hamedi, M., Halvaee, A. 2010. New parametric study of nugget size in resistance spot welding process using the finite element method, Mater. Des., 31, pp. 149-157, 10.1016/j.matdes.2009.06.042

[36] Ünlükal, E. 2007. Otomotiv Sanayinde Kullanılan Direnç Nokta Kaynak Kalitesinin Artırılması, Master Thesis, Bursa.

[37] Akyol, M. 2001. Otomotiv Sanayiinde Kullanılan Direnç Nokta Kaynak Uygulamaları ve Karşılaşılan Sorunlar, İ.T.Ü. Fen Bilimleri Enstitüsü, Master Thesis, İstanbul.

[38] Saleem, J., Majid, A., Bertilsson, K., Carlberg, T., Islam, N. 2012. Nugget Formation during Resistance Spot Welding using Finite Element Model, International Journal of Mechanical and Mechatronics Engineering, World Academy of Science, Engineering and Technology, vol. 67(7). 1228 – 1233.

[39] Rathbun, R.W., Matlock, D., Speer, J.G. 2003. Fatigue Behavior of Spot Welded High-Strength Sheet Steels. Welding Journal (Miami, Fla). 82. 207/S-218/S.

[40] Guennec, B., Akira, U., Tatsuo, S., Masahiro, T., Yu, I. 2013.s Effect of Loading Frequency in Fatigue Properties and Micro-Plasticity Behaviour of JIS S15C Low Carbon Steel, 13th International Conference on Fracture, 16–21 June, Beijing, China.

[41] Mirzaei, F., Ghorbani, H., Kolahan, 2017. F. Numerical modeling and optimization of joint strength in resistance spot welding of galvanized steel sheets. Int. J. Adv. Manuf. Technol. 92, 3489–3501.

[42] Pouranvari, M., Abedi, A.,Marashi, P., Goodarzi, M. 2008. Effect of expulsion on peak load and energy absorption of low carbon resistance spot welds. Science and Technology of Welding & Joining. 13. 39-43. 10.1179/174329307X249342.

[43] Kocabekir, B., Kaçar, R., Gündüz, S., Hayat, F. 2008. An effect of heat input, weld atmosphere and weld cooling conditions on the resistance spot weldability of 316L austenitic stainless steel. Journal of Materials Processing Technology. 195. 327-335. 10.1016/j.jmatprotec.2007.05.026.

[44] Shen, J., Zhang, Y., Wang, P.C. 2011. Nugget shifting in resistance spot welding of multi-stackup sheets. Quarterly Journal Of The Japan Welding Society. 29. 133s-137s. 10.2207/qjjws.29.133s.

[45] Khodabakhshi, F., Kazeminezhad, M., Kokabi, A. H. 2011. Mechanical properties and microstructure of resistance spot welded severely deformed low carbon steel. Materials Science and Engineering A-structural Materials Properties Microstructure and Processing - Mater Sci Eng A-Struct Mater. 529. 237-245. 10.1016/j.msea.2011.09.023.